Journal of Molecular Structure 1211 (2020) 128057

Contents lists available at ScienceDirect

Journal of Molecular Structure

journal homepage: http://www.elsevier.com/locate/molstruc

Synthesis, spectral, structure and computational studies of novel transition Metal(II) complexes of (Z)-((dimethylcarbamothioyl)thio) ((1,1,1-trifluoro-4-(naphthalen-2-yl)-4-oxobut-2-en-2-yl)oxy)

Adesoji A. Olanrewaju [a, *], Festus S. Fabiyi [a], Collins U. Ibeji [b, c, **], Emmanuel G. Kolawole [a], Rajeev Gupta [d]

[a] Department of Chemistry and Industrial Chemistry, Bowen University, Iwo, Nigeria
[b] Department of Pure and Industrial Chemistry, University of Nigeria, Nsukka, Nigeria
[c] Catalysis and Peptide Research Unit, School of Health Sciences, University of KwaZulu-Natal, Durban, 4041, South Africa
[d] Department of Chemistry, University of Delhi, Delhi, 110007, India

ARTICLE INFO

Article history:
Received 22 October 2019
Received in revised form
29 February 2020
Accepted 11 March 2020
Available online 13 March 2020

Keywords:
Synthesized complexes
Spectroscopic techniques
Stereochemistry
TGA analysis
Computational studies

ABSTRACT

Novel transition metal(II) complexes of (Z)-((dimethylcarbamothioyl)thio) ((1,1,1-trifluoro-4-(naphthalen-2-yl)-4-oxobut-2-en-2-yl)oxy) (M = Zn, Cu, Ni, Co, Fe and Mn) obtained from *N,N′*-dimethyldithiocarbamate (SDTC) and 4,4,4-trifluoro-1-(2-naphthyl)-1,3-butanedione (TFNB) have been synthesized and characterized by diverse analytical and spectroscopic techniques. The bonding nature, stereochemistry and chemical compositions of all the synthesized complexes were inferred from percentage metal, elemental analyses; infrared, electronic, mass spectra, conductivity, melting points, solubility and room temperature magnetic moments measurements. Cu(II) complex assumed a square-planar geometry, Mn(II), Fe(II) and Zn(II) complexes were tetrahedral while Co(II) and Ni(II) complexes are octahedral as deduced from electronic spectra and magnetic moments measurements. The infrared spectra data indicated that coordination with the metal ions in TFNB was via the carbonyl and enol oxygen atoms, while in SDTC the two sulphur atoms are involved. All the synthesized metal(II) complexes were covalent, as revealed by the conductivity measurements in dimethylformamide (DMF). The comparative TGA analysis of the metal complexes exhibit their thermal stability in the order: Zn(II) > Co(II) > Mn(II) > Fe(II) > Cu(II), while the computational studies of the complexes corroborate with the proposed structural geometries. Density functional theory (DFT) calculation showed that the complexes had low energy gap and higher tendency to interact with electron-accepting species.

1. Introduction

Great interest has been developed in coordination complexes of two-ligand systems of transition metal ions due to their improved diverse mode of binding and wide areas of applications [1].

Interestingly, they have been so functional in different fields or natural processes in the laboratory, environment and industry. They have been used as catalyst, agricultural products, biochemical substances, electro-chemical/chemical compounds, medicinal substance, and biological products [2–8]. It has been reported that coordination complexes play key roles in homogenous and heterogenous catalysis [9], water purification, analytical chemistry, metallurgy, solvent extraction, electrochemistry, photography, optical, dyestuffs and also used for the formulation and improvement of semiconductors, superconductors and pharmaceuticals [5–7].

However, metal complexes that would show exceptional properties and distinctive reactivity depend on the donor atoms or structural functional group(s) of the ligands. β-diketones and dithiocarbamates were among the promising ligands containing oxygen and sulphur donor atoms that were of good adaptability, diverse flexibility in coordination with the metal ions, and having various areas of applications. The enolic hydrogen atom in the

* Corresponding author.
** Corresponding author. Department of Pure and Industrial Chemistry, University of Nigeria, Nsukka, Nigeria.
E-mail addresses: sojylanrey2009@gmail.com, adesoji.olanrewaju@bowenuniversity.edu.ng (A.A. Olanrewaju), ugochukwu.ibeji@unn.edu.ng (C.U. Ibeji).

https://doi.org/10.1016/j.molstruc.2020.128057
0022-2860/

intramolecular hydrogen bonded keto-enol tautomerism of β-diketones can be easily replaced by a metal atom or ion and a ketonic oxygen bonded, thereby a metal complex is formed as a chelate ring [10]. Among other factors, solvent polarity and the presence and properties of substituents (either electron withdrawing groups or electron donating groups) also affect keto-enol equilibrium [11]. The direct result or importance of the occurrence of this greater enol formation is the capacity to form stable complexes with most metals or metal ions [12] that completely replace the enolic hydrogen atom in the chelate ring. The strong complexing properties [13] and wide area of applications of β-diketone derivatives and their metal complexes in organic and inorganic chemistry [14–16] have attracted great attention for several years. Various numbers of β-diketones with diverse substituents and their complexes have been synthesized, characterized and reported in literature to possess different chemical, biological, analytical, bio-chemical, pharmaceutical and catalytic properties [17–21] both in science and in industry.

In the same vein, dithiocarbamates possess the capability of stabilizing metals in a wide range of oxidation states [22] and ability to exhibit different structural resonance forms, especially with the delocalization of nitrogen unshared pair of electron to the sulphur ions (i.e from N through the CS_2 plane), which enables them to coordinate or bind with metals conveniently in different mode and function as monodentate, bidentate chelating as well as bidentate bridging ligands [23,24]. Several number of aliphatic and aromatic dithiocarbamate transition metal complexes have been synthesized, characterized and were reported to possess physical, biological, chemical and industrial applications [25–28].

Therefore, considering the uniqueness of the two ligands, we aim to investigate the improved activities of combining the two distinct ligands with some first row transition metals by determining their magnetic interactions (spin-crossover, antiferromagnetism or ferromagnetism), thermal stability, electronic states, intramolecular charge transfer energies, chemical reactivity strength (electrophilic or nucleophilic site of attack) and coordination behaviours that lead to geometry proposal through magnetic susceptibility measurement, infrared and electronic spectra, thermogravimetric analysis and density functional theory calculations (DFT). In connection to this, we report the synthesis, spectroscopic characterization, thermal analysis and computational studies of some 3d transition metal(II) mixed ligand complexes of *N,N′*-dimethyldithiocarbamate (SDTC) and 4,4,4-trifluoro-1-(2-naphthyl)-1,3-butanedione (TFNB).

2. Experimental

2.1. Materials

All the chemicals used (Sodium dimethyldithiocarbamic acid, 4,4,4-trifluoro-1-(2-naphthyl)-1,3-butanedione, manganese(II) sulphate monohydrate, iron(II) sulphate heptahydrate, copper(II) sulphate pentahydrate, zinc(II) sulphate heptahydrate, cobalt(II) chloride hexahydrate, nickel(II) chloride hexahydrate etc.) were of analytical grade and obtained from standard commercial groups such as Sigma-Aldrich, Central Drug House (CDH chemicals) and British Drug House Chemicals Limited (BDH). All the solvents were also used as received without further purification.

2.2. Syntheses of mixed ligand metal(II) complexes

The mixed ligand complexes of Mn(II), Fe(II), Co(II), Ni(II), Cu(II) and Zn(II) of sodium dimethyldithiocarbamate, SDTC and 4,4,4-trifluoro-1-(2-naphthyl)-1,3-butanedione, TFNB, were prepared according to published procedure [16] with little modification. Equimolar amounts of SDTC (4.19 mmol, 0.60 g) was added to a stirring solution of TFNB (4.19 mmol, 1.12 g) in 15 mL 50% ethanol at room temperature, and to the mixture were added the respective hydrated metal(II) salts (4.19 mmol, 0.71–1.20 g) in the right proportion. The resultant coloured homogenous solutions were refluxed for 5–6 h, the period which the products were produced and precipitated. The products formed were filtered, washed with ethanol and diethyl ether, then re-crystallized from ethanol and dried in *vacuo* over silica gel.

2.3. Analytical and physical measurements

The melting point/decomposition temperature of the free ligands and the mixed ligand complexes were determined with a Mel-Temp electrothermal machine while molar conductance of the complexes in DMF (1×10^{-3} M solutions) were obtained using Eutech instruments CON 510 conductivity meter. Complexometric titration method [29] was used to evaluate the percentage proportion of metals in the complexes, whereas, elemental analyses (Carbon, Hydrogen, Nitrogen, and Sulphur percentages) were recorded on Elementar Analysen Systeme GmbH Vario EL-III instrument. The solution absorption (UV–Vis) spectra of the complexes were recorded with a PerkinElmer λ 25 spectrophotometer, in the range 190–600 nm whereas infrared (IR) spectra were recorded on a SHIMADZU IR Affinity-1S FTIR spectrophotometer in the range 4000-400 cm^{-1}. Magnetic susceptibility of each of the complexes was measured on Sherwood Susceptibility Balance MSB Mark 1 at 303 (±1) K and various diamagnetic corrections were calculated using Pascal's constants [30]. ^1H and ^{13}C NMR spectra of the diamagnetic Zn(II) complex was obtained on a JEOL, JNM-ECX400Pspectrometer, using DMSO-d_6 solvent and Me_4Si internal standard. The mass spectra of the complexes were obtained on AT6530A-M(Accurate-Mass)LC-HRMS, Q-TOF components, combined with HPLC Agilent technologies 1260 Infinity and personal computer(PC).

2.4. Computational details

The ligand and metal complexes were fully optimized using Density functional theory (DFT) implemented in Gaussian 09 software [31]. B3LYP functional with 6-31 + G(d,p) basis set was applied for ligand atoms and LANL2DZ for metal ions [32]. The synergy between this functional [33] and basis sets have been reported to be suitable for compounds containing metal ions [32–34]. True energy minima were verified by performing frequency calculation for all complexes with no indication of imaginary frequencies. The scaling factor of 0.964 [35] was applied to obtain the calculated vibrational frequencies and the HOMO-LUMO orbitals was generated with iso-value of 0.02.

The second-order perturbation theory was applied to obtain the stabilization energy, E^2 *via* Natural bond orbital calculation. The donor-acceptor interactions between metals and ligand [36] were established. The E^2 calculations [37] is described by the expression:

$$E^2 = \Delta E_{ij} = q_j \frac{F(i,j)^2}{\varepsilon_j - \varepsilon_i} \quad (1)$$

where q_j is the donor orbital occupancy, ε_i and ε_j are diagonal matrix elements and $F(i,j)$ is the NBO Fock off-diagonal element.

The DFT calculation of ^1H magnetic shielding constants, with chemical shifts, obtained on a δ-scale relative to the TMS, taken as reference was performed on Zn(II) using the Gauge-Independent Atomic Orbital (GIAO) method developed by Wolinski et al. [38].

Polarizable Continuum Model (PCM) [47] through a single point (B3LYP/6-311 + G(2d,p)) calculation [39] was used for determining the ^{1}H NMR chemical shift (DMSO solvent: dielectric constant, $\varepsilon = 46.826$).

3. Results and discussion

3.1. Physical properties, analytical and elemental data

The colour, melting point, yield (% yield), percentage metal, molar conductance and elemental analysis data for the complexes were presented in Table 1. All the synthesized mixed ligand metal(II) complexes were obtained as solid in good yields within 69–85% and found to be air-stable at room temperature. The colour of ligand TFNB and Mn(II) complex are shades of yellow, Co(II) and Ni(II) complexes are of green shades while Fe(II) and Cu(II) complexes are dark-brown and grey respectively. Ligand SDTC and Zn(II) complex also possessed white and dull-white colour respectively. The complexes were expectedly coloured due to d-d transition [40].

The melting points/decomposition temperatures of all the metal(II) complexes were distinctively higher (137–206 °C) compared to the respective free ligands TFNB and SDTC melting points (72–118 °C), corroborating coordination. Furthermore, the closeness of experimental percentage metal, as well as the elemental (C, H, N, S) analyses data with their respective theoretical data of all the metal(II) complexes further established coordination. The proposed structures, formulae and composition of the metal(II) complexes were confirmed by the combination of all the analytical and spectroscopic data.

The covalent nature of the metal(II) complexes were confirmed by the molar conductance values in the range 8.68–32.60 $\Omega^{-1}cm^2mol^{-1}$ obtained in 1×10^{-3} M DMF solution, since the values were below 60 $\Omega^{-1}cm^2mol^{-1}$reported for 1:1 electrolyte [41].

3.2. Infrared spectra

The major infrared spectral vibrations of dimethyldithiocarbamate, SDTC, 4,4,4-trifluoro-1-(2-naphthyl)-1,3-butanedione, TFNB, and their complexes **13, 14, 15, 16, 17,** and **18** are presented in Table 2.

The spectra of the metal(II) complexes displayed broad bands within the region 3366-3518 cm^{-1}, assigned to OH stretching frequency due to crystallized and/or coordinated water molecule. The assignment of υ(OH) enol of ligand TNFB is due to the weak, broad band in its spectrum at 3066 cm^{-1} [42]. This band shifted in all the metal(II) complexes from 3066 cm^{-1} to 3052-3063 cm^{-1}. Moreover, coordination is observed in all of the metal(II) complexes at the carbonyl oxygen atom and C-3 enolic hydroxyl groups [43]. This is because the υ(C=O) and the υ(C–O) strong bands of the ligand $\mathbf{L^3}$, suffered bathochromic shift from 1597 cm^{-1} and 1189 cm^{-1} to 1588 - 1595 cm^{-1} and 1179 - 1191 cm^{-1} respectively [44].

The dithiocarbamate shows a band attributed to υ(C–N) at 1234 cm^{-1}, which appeared in the metal(II) complexes as an overlap of υ(C–O) bands. The appearance of sharp bands in the ligandSDTC at 960 cm^{-1} and 845 cm^{-1}, assigned to υ(C=S) and υ(C–S), shifted in all the metal(II) complexes to 952-966 cm^{-1} and 858-865 cm^{-1} respectively, an indication that the sulphur atoms coordinate to the metal ion, thus, SDTC is bidentate [24].

The bands present in the range 2906–2932 cm^{-1} were assigned due to υ(C–H) stretching vibrations of the methyl group in the ligand, SDTC and all the metal(II) complexes. The υ(M – O) and υ(M – S) bands were absent in the ligands, but they appeared in the spectra of the complexes at the range 525–583 cm^{-1} and 466 - 467 cm^{-1} respectively, confirming coordination in all the metal(II) complexes. However, these bands, υ(M – O) and υ(M – S) has been reported to be found around 419 - 586 cm^{-1} and 365 -465 cm^{-1} respectively [16,45].

3.3. Electronic spectra and magnetic moments

The substantial electronic absorption bands of **L**, $\mathbf{L^3}$ and complexes **13**–**18** were obtained in DMF as a solution absorption spectra are given in Table 3.

Generally, two main peaks characterized the electronic spectra of the compounds between 339 and 332 nm (29,499–30,120 cm^{-1}) and 300 - 267 nm (33,333–37,453 cm^{-1}), assigned to n → π* and π → π* transitions respectively. The absorption bands in the two ligands $\mathbf{L^3}$ and **L,** experienced a red shift (bathochromic shift i.e longer wavelengths) in all the metal(II) complexes due to coordination/complexation [46].

The complex **13,** showed an absorption band at 411 nm (24,331 cm^{-1}, $\varepsilon = 100$ $Lcm^{-1}mol^{-1}$), assigned to $^6A_1 \rightarrow {}^4E(G)$ transition, which was suggestive of a four coordinate tetrahedral geometry. An observed magnetic moments of 5.65–6.10 B.M is usually expected for the Mn(II) complexes at room temperature, regardless of stereochemistry since the ground term is $^6A_1$ and thus, there is no orbital contribution. In this study, the Mn(II) complex has a magnetic moment of 5.99 B.M, complementary of the proposed tetrahedral geometry [47,48].

The electronic spectrum of complex **14,** displayed an absorption band at 469 nm (21,322 cm^{-1}, $\varepsilon = 300$ $Lcm^{-1}mol^{-1}$), which indicated a four coordinate tetrahedral geometry and is assigned as $^5T_2 \rightarrow {}^5E$transition. The electronic configuration of Fe(II) is a d^6, and it has a spectroscopic ground term of ^5D. An observed magnetic moment in between 5.0 and 5.5 B.M is usually expected for high spin Fe(II) complexes and low spin complexes are expected to be

Table 1
Physical properties, analytical and elemental data of the compounds.

Compounds (Molecular formulae)	Weight (g)	Colour	Yield (% yield)	Mt. Pt/# (°C)	^M	% metal (Exp.) Theo.	Calculated (Found), %			
							C	H	N	S
TfNBD (**L^3**) $C_{14}H_9O_2F_3$	266.22	Light- yellow	–	72–74	–	- -	–	–	–	–
SDTC (**L**) $C_3H_6NS_2Na$	143.21	Off-White	–	116–118	–	- -	–	–	–	–
(13) [MnLL^3].H_2O $C_{17}H_{16}F_3MnNO_3S_2$	458.37	Yellow	1.63 (85)	144–146	8.68	11.99 (12.31)	44.55 (44.35)	3.52 (3.48)	3.06 (3.02)	13.99 14.04
(14) [FeLL^3].H_2O $C_{17}H_{16}F_3FeNO_3S_2$	459.28	Dark-brown	1.60 (83)	137–138	32.60	12.16 (11.62)	44.46 (44.36)	3.51 (3.50)	3.05 (3.15)	13.96 (13.99)
(15) [Co$LL^3(H_2O)_2$] $C_{17}H_{18}CoF_3NO_4S_2$	480.38	Teal-green	1.38 (69)	154#	10.89	12.27 (12.26)	42.51 (42.49)	3.78 (3.76)	2.92 (2.98)	13.35 (13.40)
(16)[Ni$LL^3(H_2O)_2$] $C_{17}H_{18}F_3NNiO_4S_2$	480.14	Pale-green	1.56 (78)	180–182	19.23	12.22 (12.21)	42.53 (42.58)	3.78 (3.83)	2.92 (2.89)	13.35 (13.29)
(17) [CuLL^3] $C_{17}H_{14}CuF_3NO_2S_2$	448.97	Grey	1.57 (84)	206#	19.91	14.15 (14.23)	45.48 (45.50)	3.14 (3.08)	3.12 (3.16)	14.28 (14.32)
(18) [ZnLL^3].H_2O $C_{17}H_{16}F_3NO_3S_2Zn$	468.81	Dull-White	1.66 (85)	140–142	16.89	13.95 (13.60)	43.55 (43.44)	3.44 (3.13)	2.99 (3.12)	13.68 (13.74)

Mt.pt. = Melting point, # = Decomposition temperature, % = percentage, Theo. = theoretical, Exp. = Experimental, ^M = molar conductance ($\Omega^{-1}cm^2mol^{-1}$), C = Carbon, H = Hydrogen, N = Nitrogen, S = Sulphur.

Table 2
The relevant infrared spectra data of the ligands and metal(II) complexes.

Ligands/Complexes	ν(OH) H_2O	ν(C=O)	ν(C–O)/ν(C–N)	ν(C=S/ν(C–S)	ν(O–H) enol	ν(C–F)	ν(C–H) Alkyl	ν(M – O)/ν (M – S)
TFNB (**L^3**)	–	1597s	1189s	–	3066s	1274s	–	–
SDTC (**L**)	–	–	1234s	960s/845s	–	–	2923s	–
(13) [$MnLL^3$].H_2O	3412b	1590s	1181s 1126s	952s/865s 800s	3058s	1293s	2913m	582s 466s
(14) [$FeLL^3$].H_2O	3406b	1588s	1191s 1129s	962s/863s 798s	3063m	1298s	2926m	583s 467s
(15) [$CoLL^3(H_2O)_2$]	3518b 3366b	1595s	1183s 1125s	956s/865s 795s	3060s	1299s	2916m	583s 467s
(16)[$NiLL^3(H_2O)_2$]	3509b 3367b	1605s	1183s 1127s	959s/861s 793s	3057m	1299s	2906m	583s 467s
(17) [$CuLL^3$]	–	1595s	1179s 1133s	952s/858s 785s	3052s	1299s	2932m	525s 467s
(18) [$ZnLL^3$].H_2O	3375b	1595s	1180s 1125s	966s/865s 793s	3063m	1295s	2930m	583s 467s

s = strong or sharp, b = broad, m = medium, w = weak, wb = weak-broad.

Table 3
Electronic spectra and magnetic moments data of the compounds.

Compounds	Regions of absorption nmcm$^{-1}\varepsilon$			Assignments	Assumed geometries	μeff (B.M.)
TfNBD(**L^3**)	267	37,453		π → π*	–	–
$C_{14}H_9O_2F_3$	283	35,336		π → π* n → π*		
	333	30,030				
SDTC (**L**)	267	37,453		π → π*	–	–
$C_3H_6NS_2Na$	300	33,333		π → π*		
(13) [$MnLL^3$].H_2O	285	35,088	2100	π → π* n → π*	Tetrahedral	5.99
$C_{17}H_{16}F_3MnNO_3S_2$	338	29,586	3600	$^6A_1 \rightarrow {}^4E(G)$		
	411	24,331	100			
(14) [$FeLL^3$].H_2O	331	30,211	2300	n → π*	Tetrahedral	5.30
$C_{17}H_{16}F_3FeNO_3S_2$	469	21,322	300	$^5T_2 \rightarrow {}^5E$		
(15) [$CoLL^3(H_2O)_2$]	332	30,120	7300	n → π*	Octahedral	3.80
$C_{17}H_{18}CoF_3NO_4S_2$	460	21,739	150	$^4T_{1g}(F) \rightarrow {}^4T_{1g}(P)$		
	489	20,450	90	$^4T_{1g}(F) \rightarrow {}^4A_{2g}$		
	513	19,493	70	$^4T_{1g}(F) \rightarrow {}^4T_{2g}(F)$		
(16) [$NiLL^3(H_2O)_2$]	337	29,674	690	$^3A_{2g} \rightarrow {}^3T_{1g}(P)$	Octahedral	2.35
$C_{17}H_{18}F_3NNiO_4S_2$	422	23,697	1400	$^3A_{2g} \rightarrow {}^3T_{1g}(F)$		
(17) [$CuLL^3$]	339	29,499	2200	n → π*	Square-planar	1.74
$C_{17}H_{14}CuF_3NO_2S_2$	440	22,727	300	$^2B_{1g} \rightarrow {}^2E_{1g}$		
	524	19,084	100	$^2B_{1g} \rightarrow {}^2A_{1g}$		
(18) [$ZnLL^3$].H_2O	335	29,851	7000	M→LC.T	Tetrahedral	Dia.
$C_{17}H_{16}F_3NO_3S_2Zn$						

nm = nanometer (unit of wavelength (λ)), cm^{-1} = per centimeter or reciprocal centimeter, (unit of wavenumber ($\bar{\upsilon}$), ε = Molar absorptivity ($Lcm^{-1}mol^{-1}$),M→L C.T = metal → ligand charge transfer,μeff = effective magnetic moment, Dia. = Diamagnetic, B.M. = Bohr Magneton.

diamagnetic. However, this Fe(II) complex has magnetic moment of 5.30 B.M, corroborative of its proposed tetrahedral geometry.

The complex **15** showed three bands at 513 nm (19,493 cm^{-1}, ε = 70 $Lcm^{-1}mol^{-1}$), assigned to $^4T_{1g}(F) \rightarrow {}^4T_{2g}$ (F) (υ_1); 489 nm (20,450 cm^{-1}, ε = 90 $Lcm^{-1}mol^{-1}$), assigned to $^4T_{1g}(F) \rightarrow {}^4A_{2g}$ (F) (υ_2); and 460 nm (21,739 cm^{-1}, ε = 150 $Lcm^{-1}mol^{-1}$), assigned to $^4T_{1g}(F) \rightarrow {}^4T_{1g}$ (P) (υ_3). The Co(II) has a d^7 electronic configuration, and a ground term symbol of ^4F. The magnetic moment of 3.80 B.M. obtained for this complex, was indicative of spin equilibrium (spin-crossover) between high spin and low spin octahedral geometry [49–51].

The complex **16,** was a Ni(II) complex which exhibited two absorption bands at 422 nm (23,697 cm^{-1}, ε = 1400 $Lcm^{-1}mol^{-1}$), assigned to $^3A_{2g}$ (F) → $^3T_{1g}$ (F) and 337 nm (29,674 cm^{-1}, ε = 690 $Lcm^{-1}mol^{-1}$), assigned to $^3A_{2g}$ (F) → $^3T_{1g}$ (P) transitions respectively, typical of a six coordinate high spin and low spin octahedral geometry [52]. The room temperature magnetic moments expected for a low spin and high spin octahedral nickel (II) complex is zero and 2.9–3.3 B.M. respectively. However, the observed moments for this complex under study is 2.35 B.M, which was indicative of a spin-crossover system (state of equilibrium) between the high and low spin octahedral geometry [53].

The complex **17,** gave two absorption bands at 524 nm (19,084 cm^{-1}, ε = 100 $Lcm^{-1}mol^{-1}$), assigned to $^2B_{1g} \rightarrow {}^2A_{1g}$ and 440 nm (22,727 cm^{-1}, ε = 300 $Lcm^{-1}mol^{-1}$), assigned to $^2B_{1g} \rightarrow {}^2E_{1g}$ transitions respectively, of a four coordinate square-planar geometry [54,55]. The electronic configuration of Cu(II) is d^9; thus, a spectroscopic ground state term symbol ^2D. A magnetic moment in the range 1.9–2.3 B.M, is typically noticed for mononuclear Cu(II) complexes, without stereochemistry consideration. Thus, a magnetic moment of 1.74 B.M. obtained for this copper(II) complex is complementary of a square-planar geometry [56].

The spectrum of complex **18** had a single absorption band at 335 nm (29,851 cm^{-1}, ε = 7000 $Lcm^{-1}mol^{-1}$), assigned as charge transfer transition from metal to ligand (MLCT). Since Zn(II) has a completely filled 3d orbital, no d-d transition is expected. Its diamagnetic nature confirmed the tetrahedral geometry proposed [54,57].

3.4. Mass spectra

The results of the mass spectra for the metal(II) complexes are given in Table 4.

Liquid chromatography high resolution mass spectra (LC-HRMS) of the complexes exhibit their *m/z* as single peaks, with an indication that their masses are observed as (M+1) value. The observed values were in good accord with that of the calculated masses (M) of all the complexes. The complexes **13, 14,** and **15** exhibit peak at *m/z* 459.3658 (found), 458.37 (calc.); 460.2747 (found), 459.28 (calc.) and 481.0140 (found), 480.38 (calc.) respectively.

Furthermore, the *m/z* peak at 480.3873 (found), 480.14 (calc.); 449.9880 (found), 448.97 (calc.) and 469.8657 (found), 468.81 (calc.) were attributed to complexes **16, 17** and **18** respectively.

Thus, the mass spectral studies in addition with other

Table 4
Data from the mass spectra of the complexes.

Complexes/Chemical formulae	Molecular Mass (Calculated)	Observed Mass (Experimental) M+1
(13) $[MnLL^3].H_2O$ $C_{17}H_{16}F_3MnNO_3S_2$	458.37	459.3658
(14) $[FeLL^3].H_2O$ $C_{17}H_{16}F_3FeNO_3S_2$	459.28	460.2747
(15) $[CoLL^3(H_2O)_2]$ $C_{17}H_{18}CoF_3NO_4S_2$	480.38	481.0140
(16)$[NiLL^3(H_2O)_2]$ $C_{17}H_{18}F_3NNiO_4S_2$	480.14	480.3873
(17) $[CuLL^3]$ $C_{17}H_{14}CuF_3NO_2S_2$	448.97	449.9880
(18) $[ZnLL^3].H_2O$ $C_{17}H_{16}F_3NO_3S_2Zn$	468.81	469.8657

spectroscopic measurements, corroborate the molecular formular/mass and composition of each complexes.

3.5. NMR spectra

The ^1H NMR and ^{13}C NMR were recorded in deuterated DMSO and only the diamagnetic Zn(II) mixed ligand complex **18** was determined (Tables 5a and 5b and supplementary data Fig. 1a and b). The ^1H NMR spectra gave a sharp singlet characteristic peak at 2.51 ppm (s, 6H, $-NC_2H_6$) which corresponds to the six protons of the two methyl group attached to the N atom of the SDTC moiety of the complex. The one proton attached to the C-12 contained in the β-diketone moiety of the complex showed up at a peak of 7.87 ppm.

Moreover, peaks in the region 7.56–7.85 ppm were assigned to three protons of the naphthyl ring in the TFNB moiety of the complex, other three protons appeared in the region 8.05–8.12 ppm; while the signal at 8.52 ppm established the seventh proton of the naphthyl ring in the whole complex.

The carbon-13 NMR spectra of the complex **18** exhibited signals at 45.30 ppm, assigned to C-16 and C-17 ($-NC_2H_6$) of SDTC moiety of the complex while the signal for C-12 of the β-diketone moiety appeared in the spectra at 90.74 ppm. The naphthyl ring plus the β-diketone moiety carbons showed signals at different chemical shifts, because of their different environment. The C-1, C-6, C-4 and C-14 signals appeared in the region 124.27–128.08 ppm; C-2, C-5 and C-7 in the region 128.50–129.58 ppm, whereas signals for C-9, C-8, C-3 and C-10 showed up in the region 130.28–136.20 ppm.

Furthermore, signals at 172.21, 190.39 and 197.40 ppm were ascribed to C-11, C-13 and C-15 of the whole complex respectively.

Thus, the ^1H- and ^{13}C- NMR of the Zn(II) complex corroborate the proposed structure or geometry.

3.6. Thermal analysis

The TGA plots of the complexes **13, 14, 15, 17** and **18** as obtained from a suitable and appropriate method earlier reported are shown comparatively in Fig. 2. Rates of heating were appropriately regulated at 10 °C per minute, under N_2 cloud at a stream tempo of

Table 5a
^1H NMR spectral data of the diamagnetic Zn(II) mixed-ligand complex **18** in DMSO-d_6 using TMS internal standard.

Compound	^1H NMR (δ/ppm)
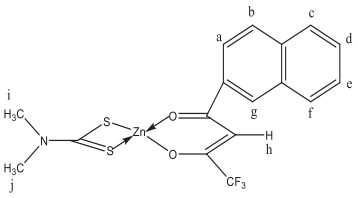	H (i & j) 2.51 = [-N(CH_3)$_2$ (6H, s)] H (h) 7.87 = [-CH (1H, s) H (d & e)7.56, 7.64 = [napht. (2H,m)] H (a) 7.85 = [napht. 1H, d] H (f) 8.05 = [napht. (1H,d)] H (c) 8.08 = [napht. (1H,d)] {3H,m} H (b) 8.12 = [napht.(1H,d)] H (g) 8.52 = [napht. (1H, s)]
(18) $[ZnLL^3].H_2O$ $C_{17}H_{16}F_3NO_3S_2Zn$	

napht. = naphthalene ring.

Table 5b
^{13}C NMR spectral data of the diamagnetic Zn(II) mixed-ligand complex **18** in DMSO-d_6 using TMS internal standard.

Compound	^{13}C NMR (δ/ppm)
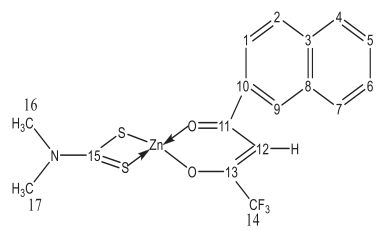	[C-16,17] = 45.30 [C-12] = 90.74 [C-1, 4, 6, & 14] = 124.27–128.08 [C-2, 5 & 7] = 128.50–129.58 [C-3, 8, 9 & 10] = 130.28–136.20 [C-11] = 172.21 [C-13] = 190.39 [C-15] = 197.40
(18) $[ZnLL^3].H_2O$ $C_{17}H_{16}F_3NO_3S_2Zn$	

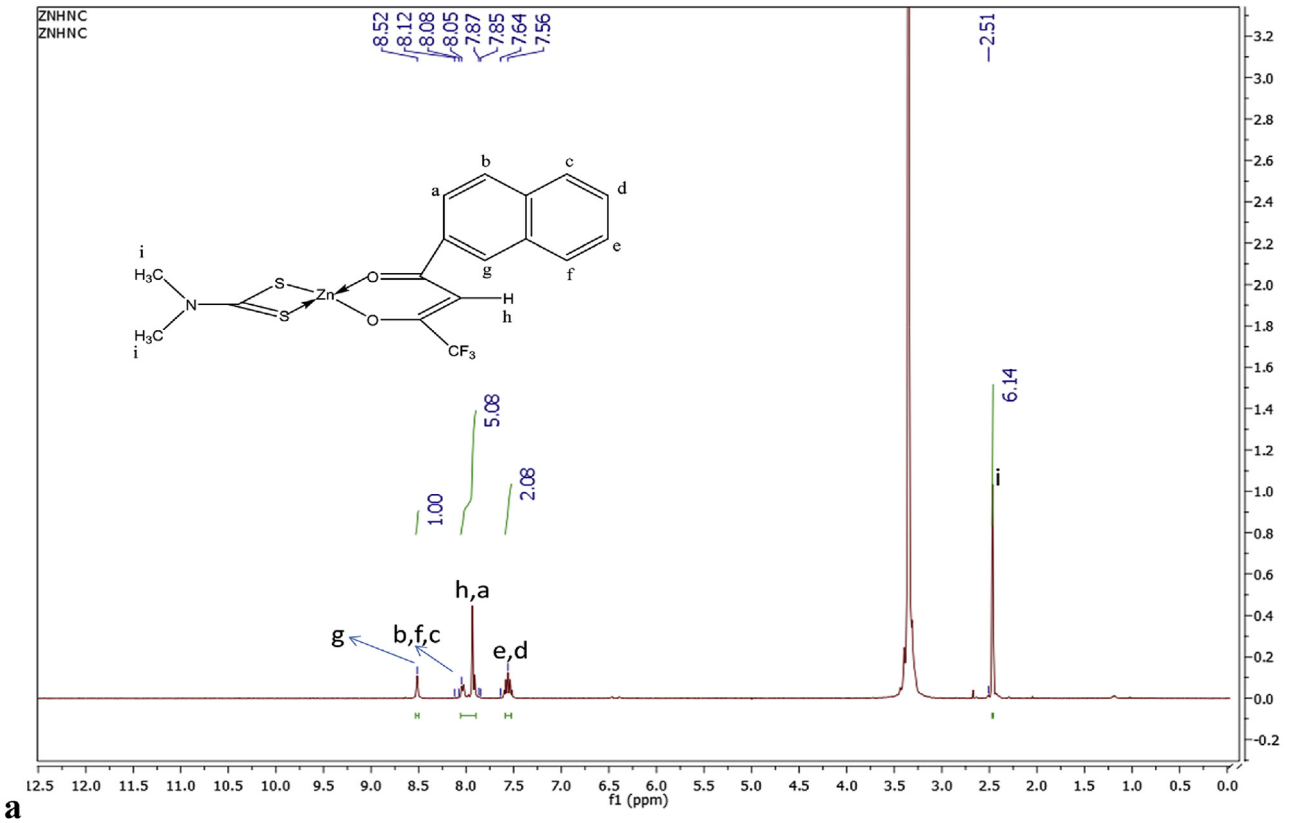

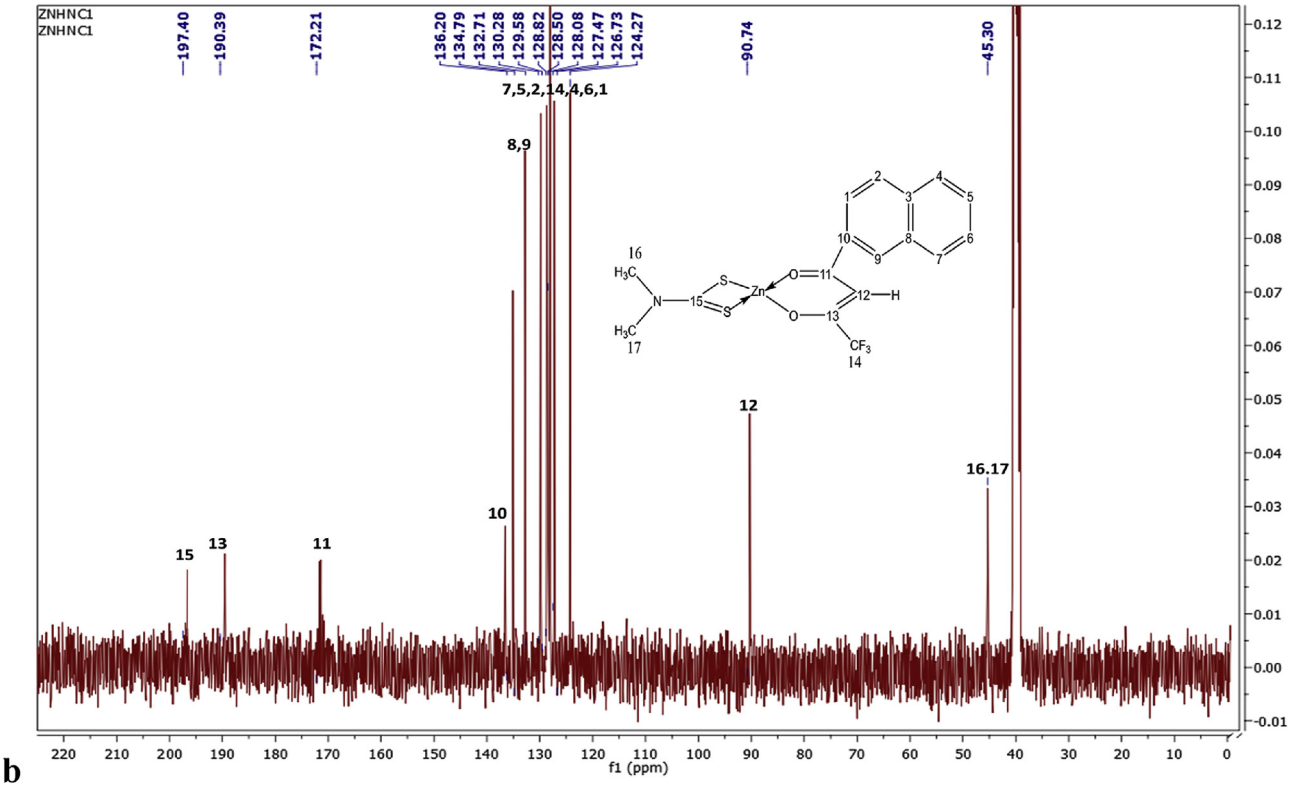

Fig. 1. a ^{1}H NMR spectra for Zn(II) mixed ligand complex **18** in DMSO-d_6. **b:** ^{13}C- NMR for Zn(II) mixed ligand complex **18** in DMSO-d_6.

200 mL/min and temperature region of 30 °C–700 °C or 800 °C.

It is crystal clear from the thermograms (Fig. 2) that each of the complexes **13, 14, 15** and **18** exhibit a three steps decomposition pattern, while complex **17** only decomposes in two steps mechanism with the loss of the two ligands, 4,4,4-trifluoro-1-(2-naphtyl)-1,3-butanedione (**L^3**) and dimethyldithiocarbamate ligand (**L**) in each step, leaving the oxide of the metal as the residue. The curves of complexes **13, 14,** and **18** show an observable change from 40 °C to 100 °C when heated, an indication of the loss of water of hydration present in them, while in complex **15**, above 100 °C, it was the loss of the coordinated water molecules. In complex **17**, the decomposition starts at about 190 °C, corroborative of absence of water of hydration. The second stage of decomposition proceeds in the temperatures range of over 100–400 °C in all the complexes, indicative of the weight loss of the ligand, L^3 and part of the ligand, L moiety. The third stage decomposition phase stand for the removal of the rest part of the ligand L moiety, at a temperature range of 400–700 °C. They are all thermally stable. Almost in all cases, the decomposition starts by the loss of crystallized/coordinated water molecule of the complexes. Mostly, the final products as residue are either oxides of the metal or metal with carbon fragment oxidized to CO_2 and nitrogen or hydrogen being lost as gases. The thermal studies of all these complexes from their curves was in good agreement with their proposed structures and their molecular formulae.

Thus, the comparative TGA curves (Fig. 2) of the metal complexes exhibit their thermal stability in the order: Zn(II) > Co(II) > Mn(II) > Fe(II) > Cu(II).

3.7. Quantum chemical studies

The optimized structures correlate with the proposed structures for the M(II) mixed ligand-complexes of TFNB and SDTC (Fig. 3). The optimized ligand and metal complexes (Fig. 4) obtained showed no negative frequencies. The bond distances between atoms and metals obtained in this study are similar to previous inter-atomic distances from our work [58] and in the literature [59,60].

3.7.1. Electronic analysis

The eigen state energies of the highest occupied molecular orbital (HOMO) and lowest unoccupied molecular orbital (LUMO) is defined by the frontier molecular orbitals [61,62]. These eigen state energies are vital in determining the chemical reactivity of compounds such as metal complexes [63,64]. The obtained HOMO, LUMO energies and dipole moment are presented in Table 6. Smaller energy gap shows that the valence electron in the HOMO can absorb lower energy and illustrate the readiness of a molecule to donate and accept electrons respectively [39]. The small ΔE gap of complex signifies higher tendencies to donate an electron to an accepting species with $[CoLL^3(H_2O)_2]$ showing a higher ability compared to other complexes. The distribution of the electron density of the HOMO describes the stability and strength of the transition metals [65].Fig. 5 reveals good stability of all complexes with regards to the complex formation based on the delocalization of the electron density around the HOMO orbital. High dipole moment favours better dipole-dipole interactions with biological systems [39]. Table 6 showed that all complexes are high dipole systems with $[ZnLL^3].H_2O$ and $[MnLL^3].H_2O$ complexes displaying stronger dipole-dipole moments compared to other metal complexes suggesting they will show better interaction with dipole moment species, especially biological systems [39]. The stability results obtained from the dipole moment agrees with the experimental results obtained for TGA analysis.

3.7.2. Electrostatic potential (EP) analysis

The Electrostatic potential at a specified zone of a compound refers to the interaction energy between an electrical charge gotten from the electrons, nuclei and proton of a molecule located at *r* [92,93]. $V(r)$ was gotten from the expression:

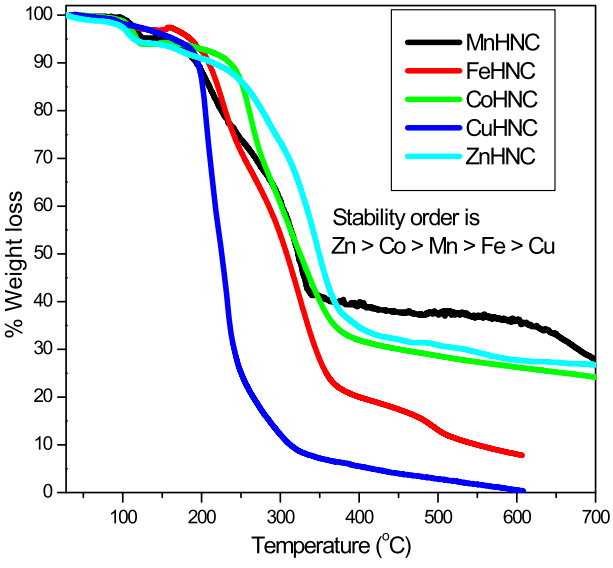

Fig. 2. Comparative TGA curves of complexes **13**–**15, 17 and 18** showing their order of stability.

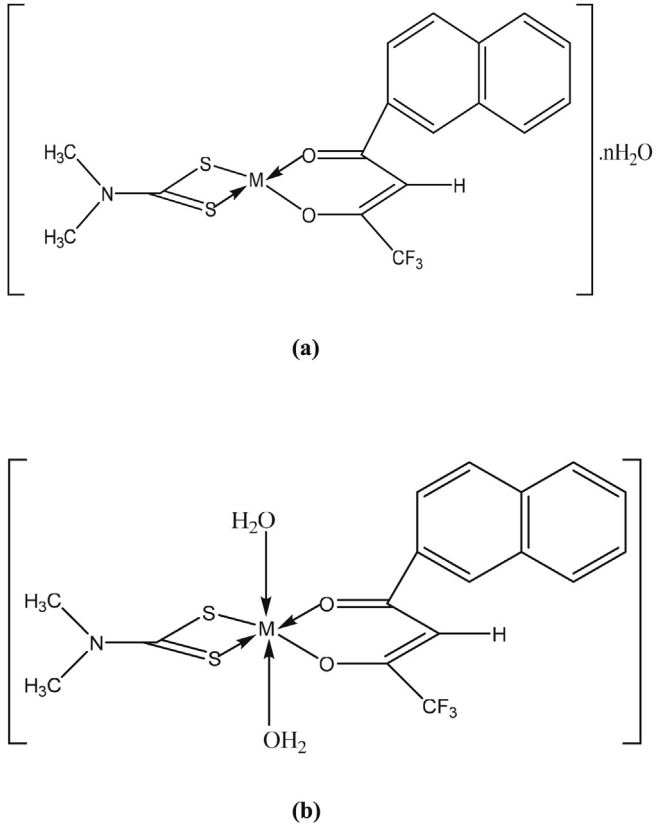

Fig. 3. The proposed structures for the M(II) mixed ligand complexes of TFNB and SDTC {**(a)** M = Mn, Fe and Zn when n = 1 respectively, and M = Cu when n = 0. **(b)** M = Co or Ni}.

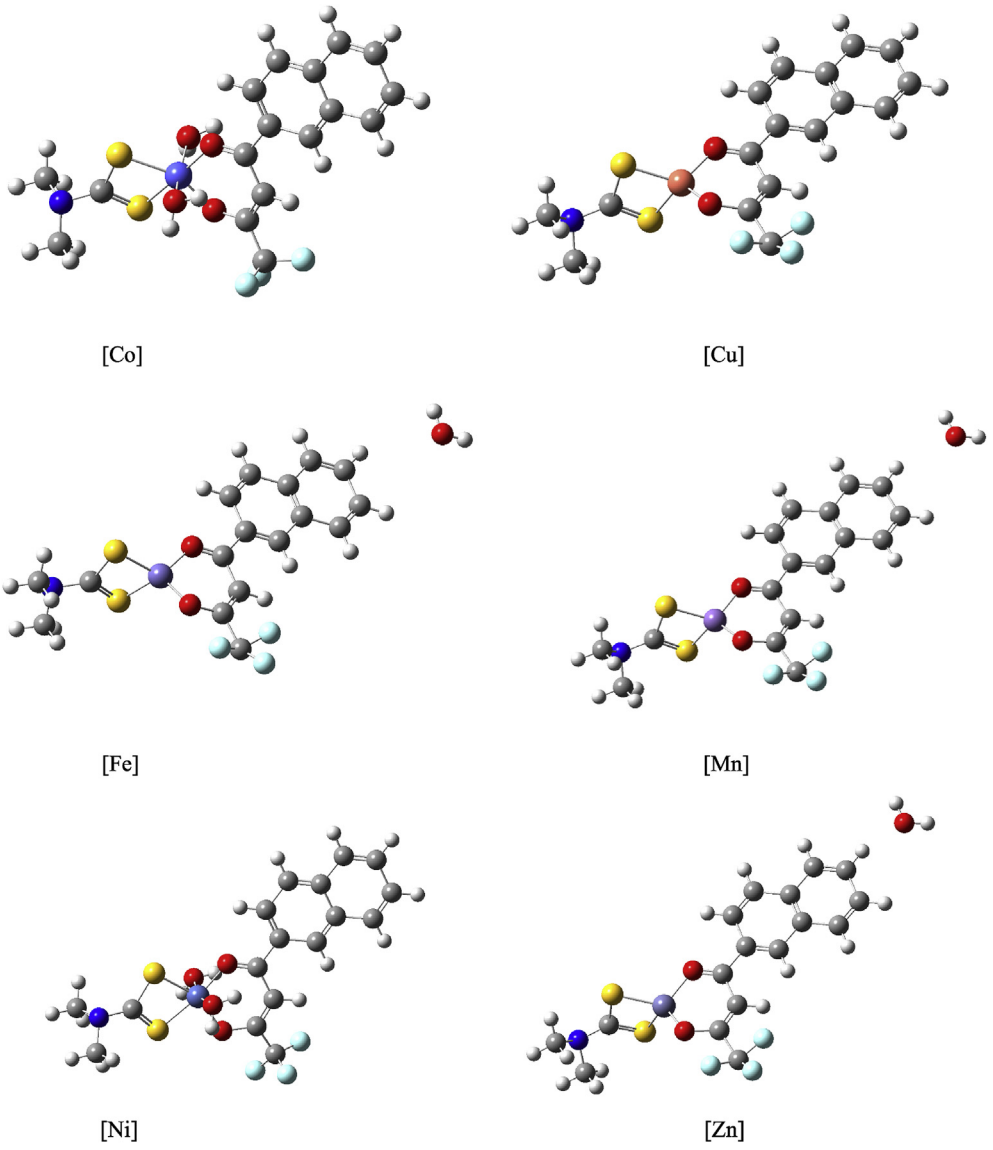

Fig. 4. Optimized geometries of metal complexes obtained at B3LYP/6-31 + G (d,p)/LANL2DZ for metal ions.

Table 6
The HOMO-LUMO, ΔE, and dipole moment of metal complexes obtained by B3LYP/6-31 + G (d,p) and LANL2DZ for metal ions.

Complex	E_{LUMO} (eV)	E_{HOMO} (eV)	ΔE (eV)	Dipole moment (Debye)
$[CoLL^3(H_2O)_2]$	−5.32	−5.50	0.18	3.3
$[MnLL^3].H_2O$	−3.65	−4.02	0.37	9.4
$[FeLL^3].H_2O$	−4.87	−5.29	0.42	4.4
$[CuLL^3]$	−5.06	−5.32	0.26	3.8
$[ZnLL^3].H_2O$	−5.26	−5.52	0.26	13.7
$[NiLL^3(H_2O)_2]$	−3.53	−4.01	0.48	6.8

$$V(r) = \sum_A \frac{Z_A}{(R_A - r)} - \int \frac{\rho(r')}{|r' - r|} dr' \quad (2)$$

Z_A represent the charge of the nucleus A located at R_A, $\rho(r')$ is the electron density function of the molecule and (r') is the dummy integration variable.

The ESP typically plays as a beneficial parameter to understand the probable site for electrophilic or nucleophilic reaction site of attack [66]. This also gives vital information about non-bonded interactions [67–69]. The electrophilic reactivity is described by the blue region of the surface (Positive electrostatic potential) while the red region signifies negative electrophilic potential associated with nucleophilic reactivity. The $V(r)$ of values associated of each complex are given in Fig. 6. The negative electrostatic potential is located around the benzene ring of all complexes. The positive ESP at the around metal ions in the complexes indicates that all complexes have the tendencies to serves as donors with $[CoLL^3(H_2O)_2]$ showing higher tendency with higher positive electrostatic potential. This observation is consistent with frontier molecular orbital describing the distribution of electron density. The red region signifies negative electrophilic potential associated with nucleophilic reactivity, negative electrostatic potential is located around benzene ring in all the complexes because it gives vital information about non-bonded interactions and the conjugated nature of the TFNB.

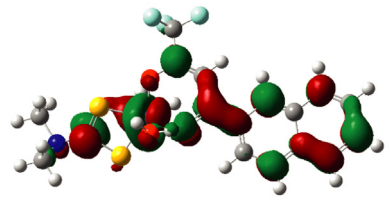

$[CoLL^3(H_2O)_2]$-HOMO

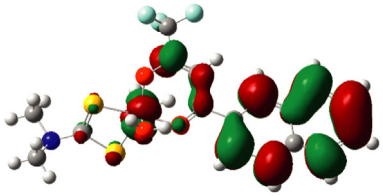

$[CoLL^3(H_2O)_2]$-LUMO

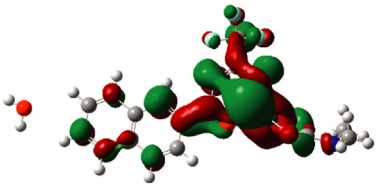

$[MnLL^3].H_2O]$-HOMO

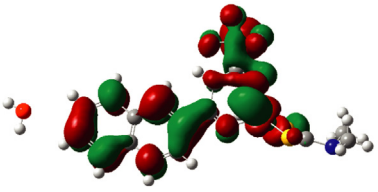

$[MnLL^3].H_2O]$-LUMO

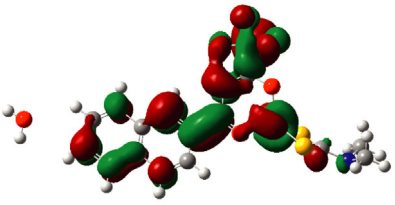

$[FeLL^3].H_2O$-HOMO

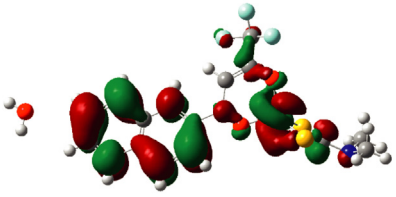

$[FeLL^3].H_2O$-LUMO

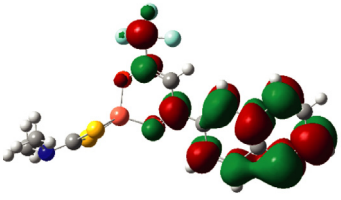

$[CuLL^3].H_2O$-HOMO

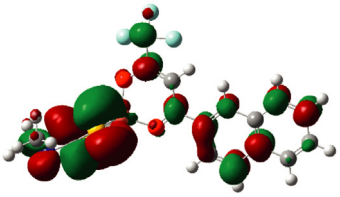

$[CuLL^3].H_2O$-LUMO

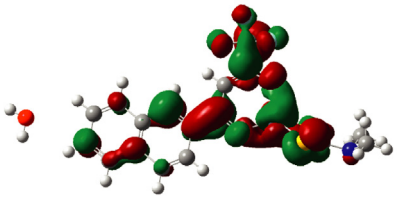

$[ZnLL^3].H_2O$-HOMO

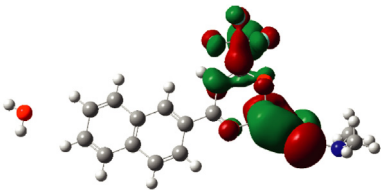

$[ZnLL^3].H_2O$-LUMO

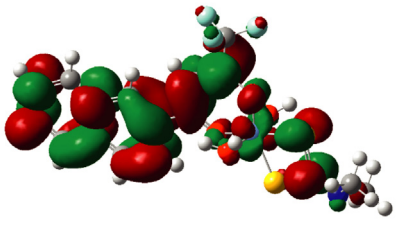

$[NiLL^3(H_2O)_2]$-HOMO

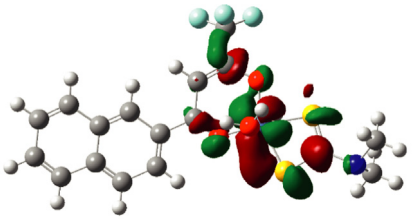

$[NiLL^3(H_2O)_2]$-LUMO

Fig. 5. Frontier molecular orbital describing the distribution of electron density for Co^{2+} and Zn^{2+}complexes obtained using B3LYP/6-31 + G (d,p)/LANL2DZ for metal ions.

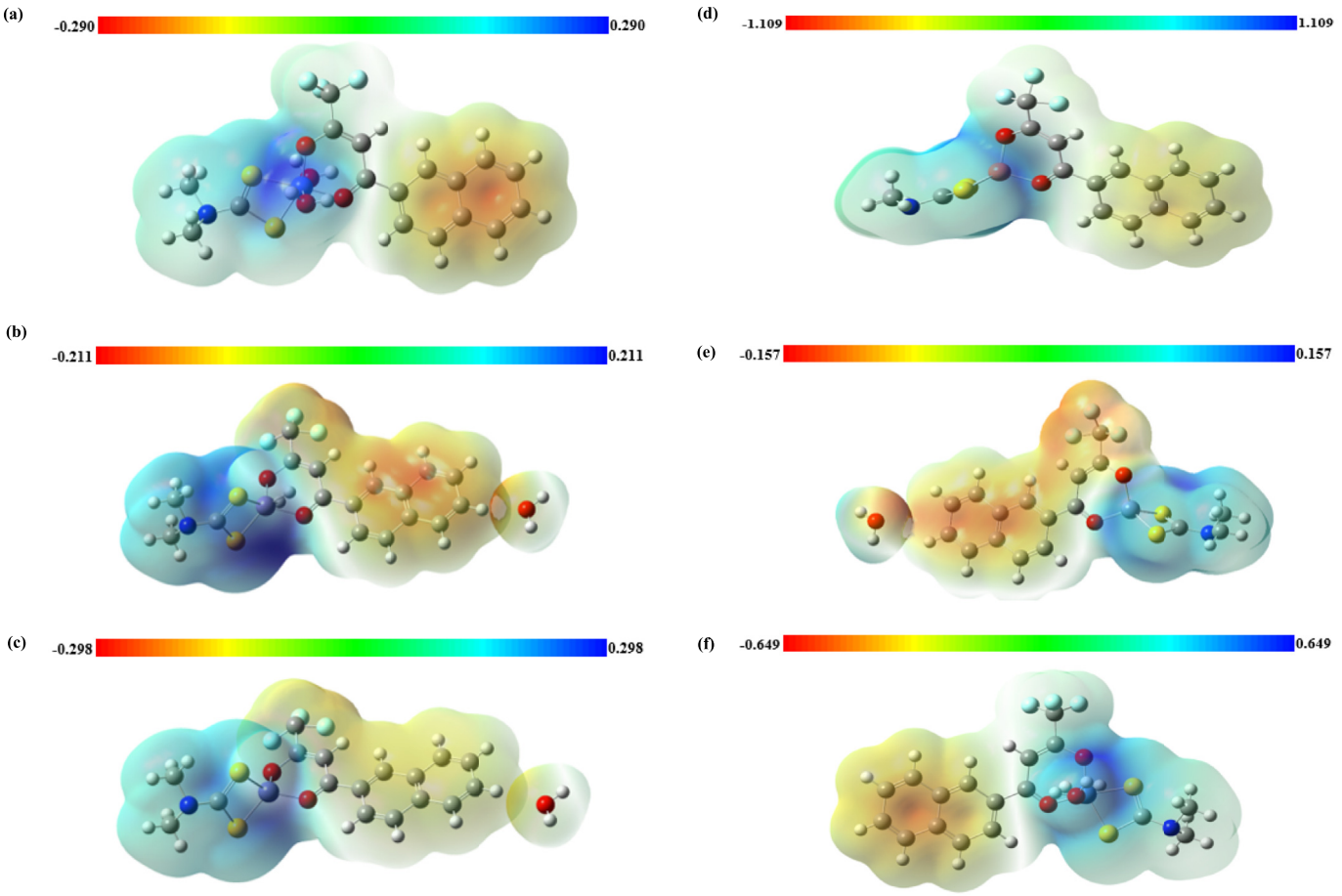

Fig. 6. Molecular electrostatic potential (MEP) map of (a) $[CoLL^3(H_2O)_2$ (b) $[MnLL^3].H_2O]$ (c) $[FeLL^3].H_2O$ (d) $[CuLL^3].H_2O$ (e) $[ZnLL^3].H_2O$ and (f) $[NiLL^3(H_2O)_2]$ complex obtained B3LYP/6-31 + G(d,p) and LANL2DZ for metal complexes.

3.7.3. ^1H NMR spectrum analysis

The theoretical ^1H NMR spectra obtained at B3LYP/6-311 + G(2d,p)-DMSO for Zn(II) is presented in the supplementary data (Figure S1). Important hydrogen atoms are indicated in the calculated ^1H NMR spectrum. Result obtained revealed good agreement with experimental ^1H NMR chemical shift, with H6 protons which corresponds to the six protons of the two methyl group attached to the N atom of the SDTC moiety of the complex showing a small deviation 0.03 ppm, except for H5 with deviation of 0.68 ppm. The reported deviation in this work is consistent with that obtained by De Souza et al. [39].

4. Conclusion

The metal(II) complexes (M = Mn, Fe, Co, Ni, Cu, Zn) of mixed ligands obtained from dimethyldithiocarbamate and 4,4,4-trifluoro-1-(2-naphthyl)-1,3-butanedione were prepared and characterized by different analytical and spectroscopic methods. From the present study, electronic and infrared spectra confirmed the octahedral geometry of Co(II) and Ni(II) chelates while other complexes adopted four-coordinate configuration systems (Cu(II) complex assumed a square-planar geometry, Mn(II), Fe(II) and Zn(II) complexes were tetrahedral) and the bidentate nature of the ligands. Non-electrolytic nature of all the metal complexes in DMF solution is established by molar conductance measurements. They were air-stable and their order of thermal stability is Zn(II) > Co(II) > Mn(II) > Fe(II) > Cu(II) as confirmed by TGA. The mass spectral and thermogravimetric analysis data confirm the structural and molecular/mass formulae proposed for all the complexes.

The computational studies corroborated the proposed structures and good stability of all complexes with regards to the complex formation based on the delocalization of the electron density around the HOMO orbital. It also establishes the good complex-target interactions of the complexes with significant binding potentials and their high dipole moment which favours better dipole-dipole interactions with biological systems.

Declaration of competing interest

The authors declare that we all worked together, agreed on the manuscript and there is no conflict of interest.

CRediT authorship contribution statement

Adesoji A. Olanrewaju: Conceptualization, Data curation, Formal analysis, Investigation, Methodology, Writing - original draft, Writing - review & editing. **Festus S. Fabiyi:** Supervision. **Collins U. Ibeji:** Methodology, Software, Validation, Visualization, Writing - original draft, Writing - review & editing. **Emmanuel G. Kolawole:** Supervision. **Rajeev Gupta:** Supervision, Project administration, Resources.

Acknowledgements

The authors appreciate effort of Professor A. A. Osowole (departed) of University of Ibadan in this research and

acknowledged Bowen University, Iwo, Nigeria and University of Delhi, India for their respective opportunity to execute the research and facilities provided. C.U.I thank CHPC (www.chpc.ac.za) and University of KwaZulu-Natal, Durban for operational and infrastructural support.

Appendix A. Supplementary data

Supplementary data to this article can be found online at https://doi.org/10.1016/j.molstruc.2020.128057.

References

[1] A.A. Olanrewaju, C.U. Ibeji, F.S. Fabiyi, Synthesis, Characterization and Computational studies of metal(II) complexes derived from β-diketone and para-aminobenzoic acid, Indian J. Heterocycl. Chem. 28 (3) (2018) 351–361.
[2] M. Ashiq, M. Danish, M.A. Mohsin, S. Bari, F. Mukhtar, Chemistry of platinum and palladium metal complexes in homogeneous and heterogeneous catalysis: a mini review, Int. J. Sci. Basic Appl. Res. 7 (1) (2013) 50–61.
[3] A. Ramadevi, K. Srinivasan, Agricultural solid waste for the removal of inorganics: adsorption of mercury (II) from aqueous solution by tamarind Nt carbon, Res. J. Chem. Environ. 12 (4) (2005) 407–412.
[4] M.B. Halli, V.B. Patil, R.B. Sumathi, K. Mallikarjun, Synthesis, characterization and biological activity of mixed ligand metal (II) complexes derived from benzofuran-2-carbohydrazide Schiff base and malonyldihydrazide, Der Pharma Chem. 4 (6) (2012) 2360–2367.
[5] Y. Aydogdu, E. Yakuphanoglu, A. Aydogdu, E. Tas, A. Cukurovali, Solid state electrical conductivity properties of copper complexes of novel oxime compounds containing oxolane ring, Mater. Lett. 57 (24) (2003) 3755–3760.
[6] J. Fisher, R. Potter, C. Barnard, Application of coordination complexes: review, Platin. Met. Rev. 48 (3) (2004) 101–104.
[7] T. Matsukura, H. Tanaka, Applicability of zinc complex of L-carnosine for medical use, Biochemistry (Mosc.) 65 (7) (2000) 817–823.
[8] V.L. Siiji, M.R. Sudarsanakumar, S. Suma, M.R.P. Kurup, Synthesis, characterization and physicochemical information, along with antimicrobial studies of some metal complexes derived from an ON donor semicarbazone ligand, Spectrochim. Acta: Mol. Biomol. Spectrosc. 76 (1) (2010) 22–28.
[9] H. Willms, W. Frank, C. Ganter, Coordination chemistry and catalytic application of bidentate phosphoferrocene -pyrazole and -imidazole based P, N-ligands, Organometallics 28 (10) (2009) 3049–3058.
[10] S.F. Tayyari, F. Milani-Nejad, H. Rahemi, Structure and vibrational spectra of the enol form of hexafluoro-acetylacetone. A density functional theoretical study, Spectrochim. Acta, Part A 58 (2002) 1669–1679.
[11] A. Manuel, R. Silva, L.M. Santos, Standard molar enthalpies of copper(II) β-diketonates and monothio- β-diketonates, J. Chem. Thermodyn. 38 (7) (2006) 817–824.
[12] W. Urbaniak, K. Jurek, K. Witt, A. Gorączko, B. Staniszewski, Properties and application of diketones and their derivatives, CHEMIK 65 (4) (2011) 273–282.
[13] C.H. Huang, K. Wang, Rare Earth Coordination Chemistry, John Wiley & Sons (Asia) Pte Ltd, 2010, pp. 41–85, 2 Clementi Loop, Singapore.
[14] J.J. Wilson, S.J. Lipparad, In vitro anticancer activity of cis-diammine platinum(II) complexes with β-diketonate leaving group ligands, J. Med. Chem. 55 (2012) 5326–5336.
[15] J.C. Almeida, I.M. Marzano, F.C. Silva de Paula, M. Pivatto, N.P. Lopes, P.C. de Souza, F.R. Pavan, A.L.B. Forminga, E.C. Pereira-Maia, W. Guerra, Complexes of platinum and palladium with B-diketones and DMSO: synthesis, characterization, molecular modeling, and biological studies, J. Mol. Struct. 1075 (2014) 370–376.
[16] A.C. Ekennia, D.C. Onwudiwe, L.O. Olasunkanmi, A.A. Osowole, E.E. Ebenso, Synthesis, DFT calculation, and antimicrobial studies of novel Zn (II), Co(II), Cu(II), and Mn(II) heteroleptic complexes containing benzoylacetone and dithiocarbamate, Bioinorgan. Chem. Appl. 2015 (2015) 1–10.
[17] A.Z. El-Sonbati, M.A. Diab, A.A. Belal, S.M. Morgan, Supramolecular structure and spectral studies on mixed-ligand complexes derived from β-diketone with azodye rhodanine derivatives, Spectrochim. Acta 99 (2012) 353–360.
[18] D.F. Xu, Z.H. Shen, Y. Shi, Q. He, Q.C. Xia, Synthesis, characterization, crystal structure, and biological activity of the copper complex, Russ. J. Coord. Chem. 36 (2010) 458–462.
[19] T. Schroeder, V. Ugrinova, B.C. Noll, S.N. Brown, A chelating β-diketone/phenoxide ligand and its coordination behavior toward titanium and scandium, Dalton Trans. 8 (2006) 1030–1040.
[20] K. Krishnankutty, V.D. John, G.J. Kuttan, Anti-tumor studies of metal chelates of synthetic curcuminoids, J. Exp. Clin. Canc. Res. 21 (2) (2002) 219–224.
[21] W.R. Cullen, E.B. Wickenheiser, Rhodium(I) complexes of β-diketonates and related ligands as hydrosilylation catalysts, J. Organomet. Chem. 370 (1989) 141.
[22] A. Jayaraju, M.M. Ahamad, R.M. Rao, J. Sreeramulu, Synthesis, characterization and biological evaluation of novel dithiocarbamate metal complexes, J. Der Pharma Chem. 4 (2012) 1191–1194.
[23] M.M. Ahamad, R.M. Rao, E.V.S. Kumar, A. Jayaraju, T.N. Begum, J. Sreeramulu, Synthesis, characterization and biological evaluation of novel dithiocarbamate metal complexes, J. Chem. Pharmaceut. Res. 4 (3) (2012) 1601–1605.
[24] D.C. Onwudiwe, P.A. Ajibade, Synthesis and crystal structure of Bis(*N*-alkyl-*N*-phenyldithiocarbamato) mercury(II), J. Chem. Crystallogr. 41 (7) (2011) 980–985.
[25] P. Villa, C. Len, A.S. Boulogne-Merlot, D. Postel, G. Ronco, C. Goubert, .H. Simon, Synthesis and antifungal activity of novel bis (dithiocarbamate) derivatives of glycerol, J. Agric. Food Chem. 44 (9) (1996) 2856–2858.
[26] T.W. Greene, P.G.M. Wuts, Protecting Groups in Organic Synthesis, third ed., Wiley Interscience, New York, 1999, p. 484.
[27] H. Pang, D. Chen, Q.C. Cui, Q.P. Dou, Sodium diethyldithiocarbamate, an AIDS progression inhibitor and a copper-binding compound, has proteasome inhibitory and apoptosis-inducing activities in cancer cells, Int. J. Mol. Med. 19 (5) (2007) 809–816.
[28] P.J. Nieuwenhuizen, Zinc accelerator complexes.: versatile homogeneous catalysts in sulfur vulcanization, Appl. Catal. Gen. 207 (1–2) (2001) 55–68.
[29] J. Basset, R.C. Denney, G.H. Jeffery, J. Mendham, Vogel's Textbook of Quantitative Inorganic Analysis, ELBS, London, UK, 1978.
[30] A. Earnshaw, The Introduction to Magnetochemistry, Academic Press, New York, NY, USA, 1980.
[31] M. Frisch, G. Trucks, H.B. Schlegel, G. Scuseria, M. Robb, J. Cheeseman, G. Scalmani, V. Barone, B. Mennucci, G. Petersson, Gaussian 09, Revision D. 01, Gaussian, Inc., Wallingford CT, 2009.
[32] A.C. Ekennia, A.A. Osowole, L.O. Olasunkanmi, D.C. Onwudiwe, O.O. Olubiyi, E.E. Ebenso, Synthesis, characterization, DFT calculations and molecular docking studies of metal (II) complexes, J. Mol. Struct. 1150 (2017) 279–292.
[33] I.A. Adejoro, D.C. Akintayo, C.U. Ibeji, The efficiency of chloroquine as corrosion inhibitor for aluminium in 1M HCl solution: experimental and DFT study, Jordan J. Chem. 11 (1) (2016) 38–49.
[34] S.I. Gorelsky, L. Basumallick, J. Vura-Weis, R. Sarangi, K.O. Hodgson, B. Hedman, K. Fujisawa, E.I. Solomon, Spectroscopic and DFT investigation of [M {HB (3, 5-i Pr2pz) 3}(SC6F5)](M= Mn, Fe, Co, Ni, Cu, and Zn) Model complexes: periodic trends in Metal– thiolate bonding, Inorg. Chem. 44 (14) (2005) 4947–4960.
[35] R.D. Johnson III, NIST 101, Computational Chemistry Comparison and Benchmark Database, 1999.
[36] F.Y. Adeowo, B. Honarparvar, A.A. Skelton, The interaction of NOTA as a bifunctional chelator with competitive alkali metal ions: a DFT study, RSC Adv. 6 (83) (2016) 79485–79496.
[37] C. James, A.A. Raj, R. Reghunathan, V. Jayakumar, I.H. Joe, Structural conformation and vibrational spectroscopic studies of 2, 6-bis (p-N, N-dimethyl benzylidene) cyclohexanone using density functional theory, J. Raman Spectrosc. 37 (12) (2006) 1381–1392.
[38] K. Wolinski, J.F. Hinton, P. Pulay, Efficient implementation of the gauge-independent atomic orbital method for NMR chemical shift calculations, J. Am. Chem. Soc. 112 (1990) 8251–8260.
[39] L.A. De Souza, W.M. Tavares, A.P.M. Lopes, M.M. Soeiro, W.B. De Almeida, Structural analysis of flavonoids in solution through DFT 1H NMR chemical shift calculations: epigallocatechin, Kaempferol and Quercetin, Chem. Phys. Lett. 676 (2017) 46–52.
[40] A.A. Olanrewaju, T.I. Oni, A.A. Osowole, Synthesis, characterization and antioxidant properties of some metal (II) complexes of mixed drugs-vitamin Bx and aspirin, Chem. Res. J. 1 (4) (2016) 90–96.
[41] A. Nagajothi, A. Kiruthika, S. Chitra, K. Parameswari, Fe(III) complexes with schiff base ligands: synthesis, characterization, and antimicrobial studies, Res. J. Chem. Sci. 3 (2) (2013) 35–43.
[42] D.L. Pavia, G.M. Lampman, G.S. Kriz, J.R. Vyvyan, Introduction to Spectroscopy, fourth ed., vol. 10, Brooks/Cole, USA, 2011, pp. 62–63. Davis Drive, Belmont, CA 94002-3098.
[43] S. Sumathi, C. Anitha, P. Tharmaraj, C.D. Sheela, Spectral, NLO, fluorescence, and biological activity of knoevenagel condensate of β-diketone ligands and their metal(II) complexes, Int. J. Integrated Care 2011 (2011) 1–8.
[44] G.B.M. Anderson, L.J. Bellamy, R.L. Williams, The infrared spectra of some gem dihydroxyl compounds and their decorated derivatives, Spectrochim. Acta 12 (1958) 233–238.
[45] T.M. Bhagat, D.K. Swamy, M.N. Deshpande, Synthesis and characterization of transition metal complexes with newly synthesized substituted benzothiazole, J. Chem. Pharmaceut. Res. 4 (2012) 100–104.
[46] S. Kumar, N. Kumar, Synthesis and biological activity of acetylacetone thiosemicarbazone and their metallic complexes, Int. Curr. Pharmaceut. J. 2 (4) (2013) 88–91.
[47] A. Saha, P. Majumda, S. Goswami, Low spin Mn(II) and Co(II) complexes of N-aryl-2-pyridylazophenylamines; New tridentate N,N,N-donors derived from cobalt mediated aromatic ring amination of 2-(phenylazo)pyridine. Crystal structure of manganese(II) complex, J. Chem. Soc., (Dalton Trans.) 11 (2000) 1703–1708.
[48] A.A. Osowole, G.A. Kolawole, R. Kempe, O.E. Fagade, Spectroscopic, magnetic and biological studies on some metal(II) complexes of 3-(4,6-Dimethyl-2 Pyrimidinyl amino)-1-Phenyl-2-Butenone and their adducts with 2,2-Bipyridine and 1,10-Phenanthroline. Synthesis and Reactivity in Inorganic, Metal-Organ. Nano-Metal Chem. 39 (3) (2009) 165–174.
[49] B.S. Manhas, B.C. Verma, S.B. Kalia, Spectral and magnetic studies on normal cobalt(II) planar and cobalt(III) octahedral, spin-crossover cobalt (III) octahedral and planar-tetrahedral cobalt(II) carbodithioates, Polyhedron 14 (23–24) (1995) 3549–3556.

[50] A.B. Gaspar, M.C. Muñoz, V. Niel, J.A. Real, [CoII (4-terpyridone) 2] X2: a novel cobalt (II) spin crossover system [4-Terpyridone=2,6-Bis(2-pyridyl)-4(1H)-pyridone], Inorg. Chem. 40 (1) (2001) 9–10.
[51] A.A. Osowole, S.M. Wakil, E.Q. Okediran, Synthesis, characterization and antimicrobial activities of some metal(II) complexes of mixed ligands-dimethyl dithiocarbamic and para aminobenzoic acids, Elixir Appl. Chem. 79 (2015) 30375–30378.
[52] S.G. Shirodkar, P.S. Mane, T.K. Chondhekar, Synthesis and fungitoxic studies of Mn(II), Co(II), Ni(II), Cu(II) with some heterocyclic Schiff base ligands, Indian J. Chem. 40A (2001) 1114–1117.
[53] H. Ma, J.L. Petersen, V.G. Young Jr., G.T. Yee, M.P. Jensen, Solid-state spin crossover of Ni (II) in a bio-inspired N_3S_2 ligand field, J. Am. Chem. Soc. 133 (15) (2011) 5644–5647.
[54] Z.H. Chohan, H. Pervez, A. Rauf, A. Scozzafava, C.T. Supuran, Antibacterial Co(II), Cu(II), Ni(II) and Zn(II) complexes of thiadiazole derived furanyl, thiophenyl and pyrrolyl Schiff bases, J. Enzym. Inhib. Med. Chem. 17 (2) (2002) 117–122.
[55] S. Chandra, K. Qanungo, S.K. Sharma, New hexadentate macrocyclic ligand and their copper(II) and nickel(II) complexes: spectral, magnetic, electrochemical, thermal, molecular modeling and antimicrobial studies, Spectrochim. Acta Mol. Biomol. Spectrosc. 94 (2012) 312–317.
[56] M.S. Mohamad, Some transition metal complexes with new Schiff base ligand hexadentate, Acta Chim. Pharmaceut. Indica 3 (2) (2013) 140–148.
[57] Z.H. Chohan, S. Kausar, Synthesis, characterization and biological properties of tridentate NNO, NNS and NNN donor thiazole-derived furanyl, thiophenyl and pyrrolyl Schiff bases and their Co(II), Cu(II), Ni(II) and Zn(II) metal chelates, Met. Base. Drugs 7 (1) (2000) 17–22.
[58] F. Chioma, A.C. Ekennia, C.U. Ibeji, S.N. Okafor, D.C. Onwudiwe, A.A. Osowole, O.T. Ujam, Synthesis, characterization, antimicrobial activity and DFT studies of 2-(pyrimidin-2-ylamino) naphthalene-1, 4-dione and its Mn (II), Co (II), Ni (II) and Zn (II) complexes, J. Mol. Struct. 1163 (2018) 455–464.
[59] B. Tang, J.-H. Ye, X.-H. Ju, Computational study of coordinated Ni (II) complex with high nitrogen content ligands, ISRN Organ. Chem. (2011) 2011.
[60] A. Nimmermark, L. Öhrström, J. Reedijk, Metal-ligand bond lengths and strengths: are they correlated? A detailed CSD analysis, Z. für Kristallogr. - Cryst. Mater. 228 (7) (2013) 311–317.
[61] C.U. Ibeji, I.A. Adejoro, B.B. Adeleke, A benchmark study on the properties of unsubstituted and some substituted polypyrroles, J. Phys. Chem. Biophys. 5 (6) (2015) 1.
[62] H.G. Kruger, Ab initio mechanistic study of the protection of alcohols and amines with anhydrides, J. Mol. Struct.: THEOCHEM 577 (2) (2002) 281–285.
[63] M.D. Diener, J.M. Alford, Isolation and properties of small-bandgap fullerenes, Nature 393 (6686) (1998) 668.
[64] C.U. Ibeji, D. Ghosh, Singlet–triplet gaps in polyacenes: a delicate balance between dynamic and static correlations investigated by spin–flip methods, Phys. Chem. Chem. Phys. 17 (15) (2015) 9849–9856.
[65] J. Griffith, L.J.Q.R. Orgel, Chem. Soc. Ligand-Field Theor. 11 (4) (1957) 381–393.
[66] C.U. Ibeji, G.F. Tolufashe, T. Ntombela, T. Govender, G.E. Maguire, G. Lamichhane, H.G. Kruger, B. Honarparvar, The catalytic role of water in the binding site of L, D-Transpeptidase 2 within acylation mechanism: a QM/MM (ONIOM) modeling, Tuberculosis 113 (2018) 222–230.
[67] A. Tokatlı, E. Özen, F. Ucun, S. Bahçeli, Quantum chemical computational studies on 5-(4-bromophenylamino)-2-methylsulfanylmethyl-2H-1, 2, 3-triazol-4-carboxylic acid ethyl ester, Spectrochim. Acta Mol. Biomol. Spectrosc. 78 (3) (2011) 1201–1211.
[68] E. Scrocco, J. Tomasi, Electronic molecular structure, reactivity and intermolecular forces: an euristic interpretation by means of electrostatic molecular potentials, Adv. Quant. Chem., Elsevier1978, pp. 115-193.
[69] F.J. Luque, J.M. López, M. Orozco, Perspective on "Electrostatic interactions of a solute with a continuum. A direct utilization of ab initio molecular potentials for the prevision of solvent effects", Theor. Chem. Accounts 103 (3–4) (2000) 343–345.